STUDY OF THE COOLING AND VACUUM SYSTEMS OF A MINIATURE 12 MeV RACE-TRACK MICROTRON *

Yu.A. Kubyshin[†], Institut de Tècniques Energètiques, UPC, Barcelona, Spain

X. Escaler, A. Viladomiu, Departament de Mecànica de Fluids, UPC, Barcelona, Spain

V.I. Shvedunov, Skobeltsyn Institute of Nuclear Physics, MSU, Moscow, Russia

Abstract

With the aim of optimization, numerical simulations of the cooling and vacuum systems of a compact 12 MeV race-track microtron (RTM) which is under construction at the Technical University of Catalonia have been carried out. The hydraulic and thermal performance of the cooling system for various flow rates has been studied using the Computational Fluid Dynamics (CFD) software. A CFD model, previously validated with experimental pressure loss results, has permitted to simulate the cooling fluid temperature, inner wall temperatures and heat transfer coefficients at different sections of the RTM accelerating structure. Conclusions concerning the current design and its possible optimization are discussed. Simulations of the RTM high vacuum conditions have been performed using the Monte-Carlo simulation package Molflow+. The pressure in the vacuum chamber, pumping tube conductance and maximum allowed throughput have been calculated. Also results of the vacuum chamber pumping out sessions are reported.

THE 12 MeV RTM AT UPC

The Technical University of Catalonia in collaboration with the Skobeltsyn Institute of Nuclear Physics of the Moscow State University and CIEMAT (Madrid) is building a compact electron accelerator of race-track microtron (RTM) type with maximal beam energy of 12 MeV. Currently, the RTM is at the final phase of its construction [1-4].

The electron beam is produced in a module called accelerator head shown in Fig. 1(a). It is a vacuum chamber that houses an electron gun, an accelerating structure (linac), two 180º bending dipoles, usually referred to as end magnets, a focusing quadrupole and four extraction dipoles.

The linac is composed of four accelerating and three coupling cells which have been brazed together to form four accelerating sections (labelled from S1 to S4) as shown in Fig. 1(b). The total power dissipated in the linac is approximately 1 kW. According to calculations of the detailed distribution of the RF power losses in the cavity walls carried out in Ref. [5] the RF power dissipated in the linac sections S1 to S4 is equal to 189.5 W, 273.7 W, 273.7 W and 263.1 W, respectively. In the magnets the magnetic field is created by REPM material, so the power dissipation in them is due to beam losses only and is estimated to be about 0.1 kW.

THE COOLING SYSTEM

In addition to the basic function of the RTM cooling system, which is to provide a safe and stable operation of all accelerator systems, it must guarantee a homogeneous temperature distribution along the linac and end magnets. In particular, the temperature differences between different parts of the linac must not exceed about ±1°C.

The cooling circuit in the accelerator head is a water pipeline passing through the end magnets and linac connected to a chiller. The chiller can provide a water mass flow rate in the range from 0.042 kg/s up to 0.075 kg/s.
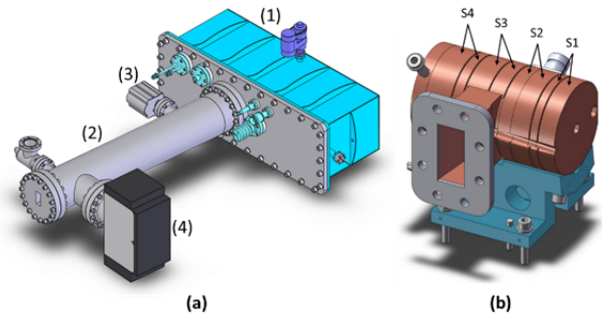

Figure 1: (a) 3D view of the RTM: (1) accelerator head, (2) vacuum tube, (3) pressure sensor, (4) ion pump. (b) 3D view of the linac with the section labels indicated.

A CFD model of the fluid domain of the RTM cooling system has been developed using the ANSYS CFX® version 14.5 [6]. The part of the cooling channels inside the linac is shown in Fig. 2. We have performed simulations of the total pressure losses and compared the result to experimental measurements [7]. For example, for the mass flow rate 0.05 kg/s the pressure loss in the accelerator head obtained in the simulations is 3.05 bar, whereas the measured value is 3.18 bar. A good agreement between these results confirms the validity of the CFD model.

COOLING SYSTEM PERFORMANCE

Using this CFD model we have carried out the thermo-fluid analysis of the cooling system for the chiller operation range. Preliminary results of have been reported in [7].

One of the results obtained in the simulations is the distribution of the cooling tube wall temperature inside the linac. As it has been already mentioned one of the critical issues is the homogeneity of the temperature along the linac. A plot of the wall temperature increase with respect to the inlet water temperature for a nominal operation regime corresponding to the mass flow rate of about

0.05 kg/s is given in Fig. 2. As one can see, the maximum increase is located in section S1. Results of simulations of the water streamlines have shown that the appearance of the region with high temperatures in the linac segment S1 is due to boundary layer detachments of the flow and low flow velocities there and, as a consequence, significant reduction of the convective heat transfer. These effects are caused by the 90º abrupt bending of the conduits in the two annular connections in this linac section.
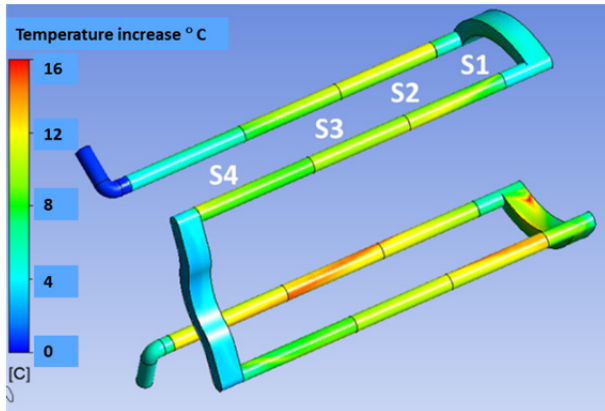

Figure 2: Wall temperature increase with respect to the inlet temperature in the linac cooling channels at the nominal mass flow rate of 0.05 kg/s.

Also the temperature inhomogeneity within each linac section has been studied. For the flow rates that the chiller can provide, the maximum differences of the average wall temperature between different parts of the same section are in S3, whereas the minimum ones are in S1 for any flow rate (see the plot in Fig. 3). These temperature differences range from approximately 1.8° C at the minimum mass flow rate to 0.8° C at the maximum one. Thus, the RTM design requirement, that the temperature difference between different linac sections does not exceed the limit of ±1°C is met for the flow rates close to the maximal one.
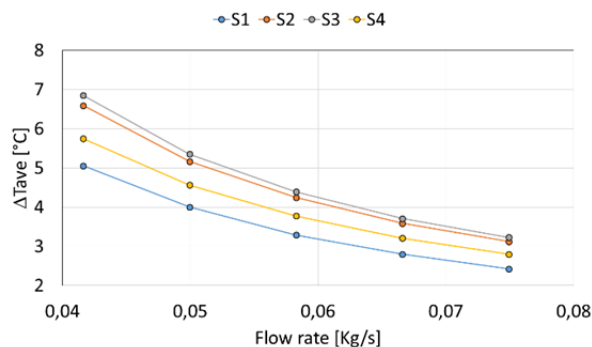

Figure 3: Average wall temperature differences relative to inlet water temperature in the linac sections as functions of mass flow rate.

THE VACUUM SYSTEM

The vacuum system of the RTM is shown schematically in Fig. 4. The vacuum chamber (1) is pumped out through the stainless steel tube (2) by a Varian VacIon *Plus* 75 Starcell ion pump (3). Inside the tube (2) a copper waveguide WR187 (4) transporting the RF power to the linac is placed. It has narrow slots at walls which facilitate the gas evacuation from the interior of the linac. The waveguide is vacuum tightly brazed to the stainless steel flange (5) and is isolated from the atmosphere by the vacuum RF window (6). The pressure in the system is measured by means of a MKS 979B atmosphere-to-vacuum transducer (7). The main valve (8) is used for disconnecting the turbomolecular pump Varian Mini-Task AG81 (9) from the pumping tube. The rest of the elements are an ISO-CF flange transition (10) and venting valves (11) and (12). The pump controllers and the vacuum transducer are connected to the RTM control system and interlocks [4].
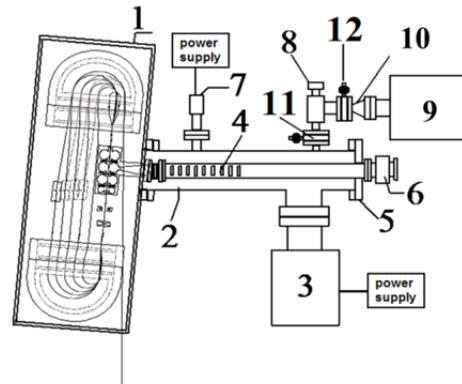

Figure 4: Schematic of the RTM vacuum system.

The nominal pumping speed of the turbomolecular and ion pumps used in the RTM vacuum system is 40 l/s and 65 l/s, respectively. First the turbomolecular pump pumps down the vacuum chamber into 10^{-5} mbar. Once this vacuum level is achieved the ion pump is switched on. After the RTM commissioning the ion pump will be permanently switched on in order to maintain a vacuum of 10^{-7} mbar in the vacuum chamber in accordance with the design specifications.

Several tests of the vacuum system have been carried out. Two example of the pressure behaviour with the pumping time are shown in Fig.5. During Session 1, a vacuum of $0.8 \cdot 10^{-7}$ mbar was achieved in about 25.5 h, and in Session 2 39.3 h were needed to reach a vacuum of $1.2 \cdot 10^{-7}$ mbar. The reason of this difference is that between these sessions the vacuum chamber was open and a number of feedthrough connectors were installed inside it.

VACUUM SYSTEM SIMULATIONS

To study the performance of the RTM vacuum system we have carried Monte-Carlo simulations of the pressure in the vacuum chamber and pumping tube using the Molflow+ program [8]. For this we developed a model shown

in Fig. 6. The main source of the outgassing was supposed to be the thermal desorption.
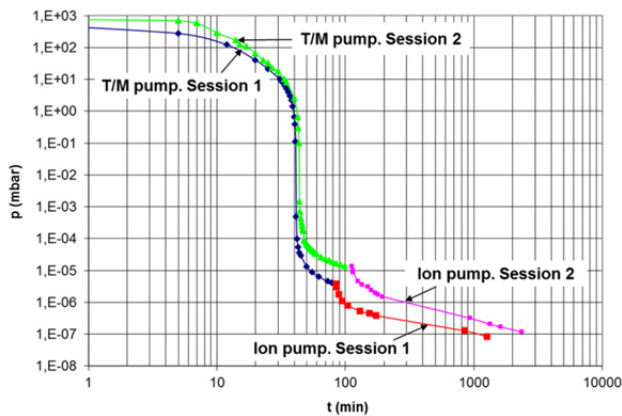

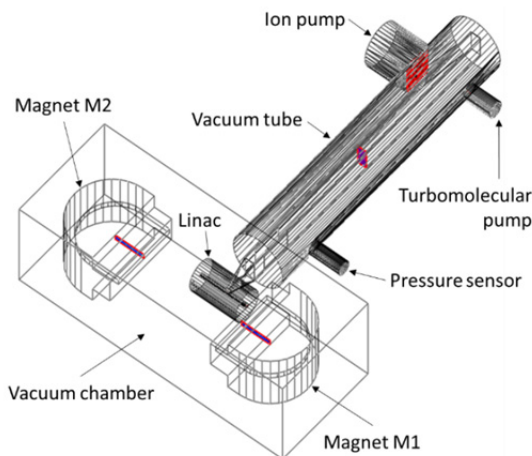Figure 5: Pressure behaviour during the vacuum system tests.

Figure 6: 3D model of the RTM vacuum system used in the simulations.

We have calculated the pressure in the equilibrium state at points critical for the beam, like the gap of the magnets and linac central channel, and also at the vacuum transducer and at the ion pump flange. For example, for the outgassing rate $q = 2 \cdot 10^{-7}$ Pa $\cdot$ m^3/(sec $\cdot$ m^2) and the pumping speed $S_p = 45$ l/s we have obtained (for N$_2$) that the pressure at the vacuum chamber flange and the ion pump flange are equal to $p_1 = 1.04 \cdot 10^{-7}$ mbar and $p_2 = 0.87 \cdot 10^{-7}$ mbar , respectively.

Using this result one can calculate the conductance of the pumping tube, namely the long tube (2) and the short tube connecting it to the ion pump (see Fig. 4). Using the standard definition (see for example Ref. [9]) it is easy to get that the conductance $C_{tube} = 221$ l/s . For the sake of comparison, an estimate of this value can be obtained using formulas for round tubes in the case of the molecular flow regime [9]. One gets that the conductance of long tube with the waveguide inside and the one of the short tube are $C_1 = 415$ l/s and $C_2 = 578$ l/s, respectively, so that the assembly conductance is approximately 242 l/s.

Finally, we have estimated the maximal gas throughput Q_{max} for which the ion pump can maintain the vacuum 10^{-7} mbar in the vacuum chamber. Using the results of the simulations for the pumping speed $S_p = 45$ l/s we have obtained $Q_{max} = 4.0 \cdot 10^{-7}$ Pa $\cdot$ m^3/sec.

CONCLUSIONS

Results of the performance of the cooling and vacuum systems of the 12 MeV RTM, obtained both experimentally and by simulations, have been discussed. It has been checked that both systems meet the design requirements and guarantee a stable operation of the machine after its commissioning.

In the case of the cooling system we have obtained that the requirement that the temperature difference between different segments of the linac does not exceed the limit of ±1° C is met for the maximal flow rate only. The geometry of the cooling channels in the linac can be optimized by filleting the surfaces at the transition between the circular pipes and the annular arms in order to create a rounded smooth transition that would help the flow to turn without detaching from the surfaces.

We have obtained an upper limit on the maximal gas throughput in the vacuum chamber with which the installed ion pump can maintain the required vacuum of 10^{-7} mbar. In order to fulfill this requirement a cleaning of the internal surfaces and baking of the chamber may be required.

REFERENCES

[1] A.P. Poseryaev, M.F. Ballester, Yu.A. Kubyshin, V.I. Shvedunov, "Design of 12 MeV RTM for Multiple Applications", *in Proc. EPAC'06*, Edinburgh, UK, June 2006, paper WEPCH175, pp. 2340-2342.

[2] Yu.A. Kubyshin et al., "Current status of the 12 MeV UPC race-track microtron", *in: Proc. PAC'09*, Vancouver, Canada, May 2009, paper WE6PFP112, pp. 2775--2779.

[3] I.Y. Vladimirov, N.I. Pakhomov, V.I. Shvedunov, Y.A. Kubyshin, J.P. Rigla and V.V. Zakharov, "End magnets with rare earth permanent magnet material for a compact race-track microtron", *Eur. Phys. J. Plus*, 129: 271, 2014.

[4] Yu.A. Kubyshin, V. Blasco, J.A. Romero, A. Sanchez, G. Montoro, and V. I. Shvedunov, Control system of a miniature 12 MeV race-track microtron", *in: Proc. IPAC'14*, Dresden, Germany, June 2014, pp. 3165--3167.

[5] D. Carrillo, "C-band linac for a race-track microtron", PhD thesis, CIEMAT, Universidad Complutense de Madrid, Spain, 2010.

[6] http://www.ansys.com/Products/Fluids/ANSYS-CFX

[7] X. Escaler, Yu.A. Kubyshin, V. Blasco, J.A. Romero, A. Sánchez, M. Prieto, and V.I. Shvedunov, "Thermo-fluid study of the UPC race-track microtron cooling system", MEDSI 2016, Barcelona, Spain, 2016.

[8] http://molflow.web.cern.ch/content/about-molflow

[9] J.F. O'Hanlon, "A User's Guide to Vacuum Technology", Wiley-Interscience, 2003.